Earth and Planetary Science Letters, 94 (1989) 385–397
Elsevier Science Publishers B.V., Amsterdam – Printed in The Netherlands

[5]

Magnetostratigraphy of the Cretaceous–Tertiary boundary at Agost (Spain)

J.J. Groot [1], R.B.G. de Jonge [1], C.G. Langereis [2], W.G.H.Z. ten Kate [1] and J. Smit [1]

[1] *Institute of Earth Sciences, Free University, P.O. Box 7161, 1007 MC Amsterdam (The Netherlands)*
[2] *Paleomagnetic Laboratory, Fort Hoofddijk, Budapestlaan 17, 3584 CD Utrecht (The Netherlands)*

Received June 7, 1988; revised version accepted June 9, 1989

A detailed magnetostratigraphic investigation of the Agost section (Spain) containing the Cretaceous–Tertiary (K/T) boundary is reported. Thermal demagnetization—contrary to alternating field demagnetization—succeeds in revealing the polarity of the characteristic remanent magnetization, although an overlap in blocking temperature spectrum exists with a normal polarity, secondary magnetization component. The K/T boundary occurs at two-thirds from the base of a reversed polarity zone and by comparison with earlier results [1] this polarity zone is correlated to chron C29r.

Linear regression of sedimentation rates in other sections with an established magnetostratigraphy and containing the K/T boundary yields an age of 66.45 Ma for this boundary. On the basis of this age and the magnetic reversal ages of the Berggren et al. [13] polarity time scale, new first appearance (FAD) ages around the K/T boundary are suggested for the planktonic species *Morozovella trinidadensis* (Bolli) (66.04 Ma), *Morozovella pseudobulloides* (Plummer) (66.34 Ma), *Eoglobigerina taurica* (Bang) (66.41 Ma) and "*Globigerina eugubina*" Luterbacher & Premoli Silva (66.43 Ma).

1. Introduction

The Cretaceous–Tertiary boundary (K/T) is at present one of the foremost topics in geology, not in the least because of the impact hypothesis of the mass extinction of species [2,3].

There are a number of continuous K/T boundary sections in Europe with an established magnetostratigraphy. A well known one is the Gubbio section [1] which has been proposed as the reference section for the magnetostratigraphy of the Late Cretaceous–Early Paleocene [4]. Other

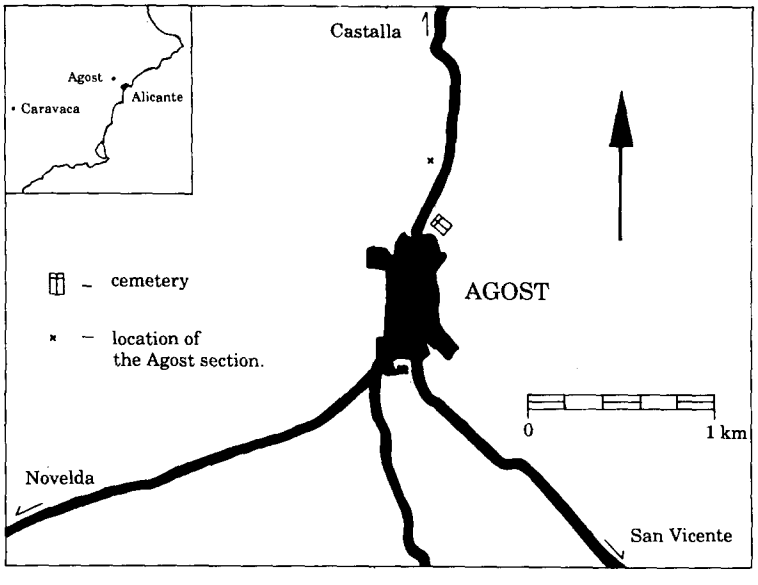

Fig. 1. Location of the Agost section.

0012-821X/89/$03.50

examples are the Zumaya section [5] and the Caravaca section [6].

The Agost section has first been described by von Hillebrandt [7], who did not analyze the K/T boundary transition. Paleogeographically, the Agost section is located on the outer shelf of the Spanish Meseta (Fig. 1). It belongs to a stratigraphic/tectonic unit intermediate between the Prebetic and Subbetic Units of the Betic Cordilleras [8]. Lithologically it is almost identical, bed to bed, to the Caravaca section [6]. It is the purpose of this paper to describe the magnetostratigraphy of the Agost section, to compare the section with other complete K/T sections, and to discuss its importance for the biogeochronology and the K/T boundary events. Detailed biostratigraphic, geochemical and mineralogical results will be published elsewhere (de Jonge et al., in preparation; Smit et al., in preparation).

2. Geologic setting and sampling

The section is developed in the so-called "Couches Rouges"-facies and consists of open-marine, hemipelagic grey to cream-coloured marls, which turn to more greyish in the Paleocene. In the marls, a few turbidites and a number of marly limestone beds are intercalated. A fault disturbs the uppermost part of the section (Fig. 8). The K/T boundary is marked by a 1–2 mm thick green clay stratum which shows a strong iridium anomaly (27 ppb; Smit et al., in preparation). The clay of this stratum is composed of almost pure smectite and contains numerous 50–700 μm sized microtektite-like spherules with an internal fibrous or dendritic mineralogical texture. These spherules are composed of K-feldspar, smectite or goethite, supposedly diagenetically altered from a precursor mineral quenched at high temperatures. This stratum is followed by a 6.5 cm thick marly clay which lacks the typical Cretaceous Globotruncana–Rugoglobigerina fauna (de Jonge et al., in preparation).

Sampling was done at an average interval of ca. 50 cm, depending on where the lithology was suitable for drilling. For magnetostratigraphic purposes, at each level several cores of 25 mm diameter were taken with an electric drill using water under pressure for cooling and a portable generator as power supply. The cores were cut into 22 mm long specimens at the paleomagnetic laboratory, Fort Hoofddijk. For biostratigraphic research, handsamples were taken, while the interval at the K/T boundary was sampled in more detail (ca. 1-cm intervals).

Stratigraphic distance between the sampling levels was accurately determined using vertical and horizontal distance and azimuth between sites as well as strike and dip (with an average of N 150°, W 24°) of the bedding plane [9]. We also used a theodolite to determine the overall stratigraphic thickness and as a check on the total inter-sample distances.

3. Biostratigraphy

The samples (57) taken for biostratigraphic research were dried and weighed before washing over a 40 μm sieve. In order to calculate planktonic foraminiferal production rates the dried residues were weighed again (de Jonge et al., in preparation). From each sample a minimum of 300 randomly chosen individuals were determined. After that, the samples were scanned for the presence of species in low abundages. A detailed biozonation of the Agost section could be established in which a total of seven planktonic foraminiferal zones were recognized (Fig. 2).

The base of the *Abathomphalus mayaroensis* Zone which is characterized by the first appearance datum (FAD) of *A. mayaroensis* (Bolli) is not reached in this section; the last appearance datum (LAD) of *A. mayaroensis*, Globotruncana and Rugoglobigerina is recorded at 11.47 m. The *A. mayaroensis* Zone contains a fauna rich in planktonic foraminifera. Thirty-two species were recognized, among those 12 Globotruncana species and 15 Heterohelicidae species. At the 11.47 m level most of these species disappear. Only *Guembelitria cretacea* survives the K/T boundary events and occurs in all samples of the section. The extinction of these foraminiferal species has been attributed to the consequences of a large impact event [2,3] and the level at which this extinction occurs is considered as the K/T boundary.

The first zone in the Tertiary is the *Guembelitria cretacea* Zone which is characterized by an abundance peak of *Guembelitria cretacea* Cushman and extends over 6.5 cm, from 11.47 to

Agost section (this paper)		Smit & Romein, 1985			Berggren et al., 1985		
Morozovella uncinata	P2	Globorotalia uncinata	P2		Morozovella uncinata	P2	
Morozovella trinidadensis	P1d	Globorotalia trinidadensis	P1d		Subbotina trinidadensis	P1	c
Morozovella pseudobulloides	P1c	Globorotalia pseudobulloides	P1c		Subbotina pseudobulloides		b
Eoglobigerina taurica	P1b	Eoglobigerina taurica	P1b		Eoglobigerina eugubina		a
'Globigerina' eugubina	P1a III	'Globigerina' eugubina	P1a	III			
		'Globigerina' fringa		II			
		'Globigerina' minutula		I			
Guembelitria cretacea	P0	Guembelitria cretacea	P0				
Ambathomphalus mayaroensis	UC17	Ambathomphalus mayaroensis	UC17		Ambathomphalus mayaroensis	UC17	

Fig. 2. Planktonic foraminiferal biostratigraphic zonation of the Agost section compared with the zonation of Smit and Romein [10] and of Berggren et al. [13].

11.535 m. No other planktonic foraminifera were recognized throughout the entire zone, except *Globotruncanella* and *Globigerinelloides* and a few heterohelicids. These genera seem to survive the main extinction event at the K/T boundary for a short (about 5–15 ka) time.

The first Tertiary species are recognized at 11.535 m. These include "*Globigerina eugubina* Luterbacher & Premoli Silva, "*Globigerina*" *minutula* Luterbacher & Premoli Silva, and "*Globigerina*" *fringa* Subbotina and they mark the lower boundary of the "*Globigerina*" *eugubina* Zone. The marker species of the *Eoglobigerina taurica* and *Morozovella pseudobulloides* Zones were first recorded at 11.69 and 12.35 m, respectively.

The base of the *Morozovella trinidadensis* Zone, identified by the FAD of its marker species *M. trinidadensis* Bolli, is recorded at 14.68 m. *M. trinidadensis* occurs at first in (relatively) low abundance. The top of the *M. trinidadensis* Zone is not reached in the Agost section, because at 20.12 m a fault intersects the section removing approximately 30 m of sediment. Directly above this fault, *Morozovella uncinata* has been found.

The (planktonic) biozonation found in the Agost section is as complete as in the Caravaca section. We follow the zonation of Smit [6] and Smit and Romein [10], which in its turn is based on van Hinte [11] for the Upper Cretaceous and on Hardenbol and Berggren [12] for the lower Paleocene, with the only difference that the basalmost Paleocene was subdivided in additional zones. The more recent zonation of Berggren et al. [13] is also recognized at Agost (Fig. 2), but the latter authors changed the lettering (P1c becomes P1b, and P1d becomes P1c) compared to earlier versions [12]. A diversification of P1a as proposed by Smit and Romein [10] for the lower Paleocene of the Kef section cannot be made. This is ascribed to a lower rate of sedimentation in combination

with high bioturbation, mixing the FAD of index species *"G." fringa, "G." minutula* and *"G." eugubina*.

The remaining Danian part of the section is characterized by a low diversity in species: only a few species more are added to those mentioned earlier. The assemblages of the planktonic foraminifera in the Cretaceous and Tertiary are characteristic for open-marine (sub)tropical water. The oxygen isotopes indicate that surface water temperatures vary from 21° C (δ^{18}O: −2.5‰) to 29° C (δ^{18}O: −4.0‰) at the Cretaceous–Tertiary boundary (de Jonge et al., in preparation).

4. Magnetostratigraphy

4.1. Laboratory treatment

Almost all measurements of the natural remanent magnetization (NRM) were done on a 2G Enterprises cryogenic magnetometer. The total NRM of all specimens, corrected for bedding tilt, is shown in Fig. 3. The total NRM directions show normal declinations with mainly positive inclinations. The dominating normal polarity suggests an overprint of the original directions with a recent magnetization, since earlier results have shown the K/T boundary to occur in a reversed polarity zone [1]. The NRM intensities vary in general from 0.4 to 1.3 mA/m; from the 11.5 m level (K/T boundary) upwards the NRM intensities become somewhat higher, up to 1.9 mA/m, and from the 14.5 m level they are lower again (0.2–0.7 mA/m).

In order to reveal the original NRM, at least two specimens per site were progressively demagnetized using a large number (16–22) of steps. Most specimens were demagnetized thermally in a non-magnetic furnace up to temperatures of 575° C; a number of specimens [19] were demagnetized in alternating fields, up to a maximum of 290 mT.

The Zijderveld [14] demagnetization diagrams revealed the existence of several components (Fig. 4). Generally, the first component is a small ran-

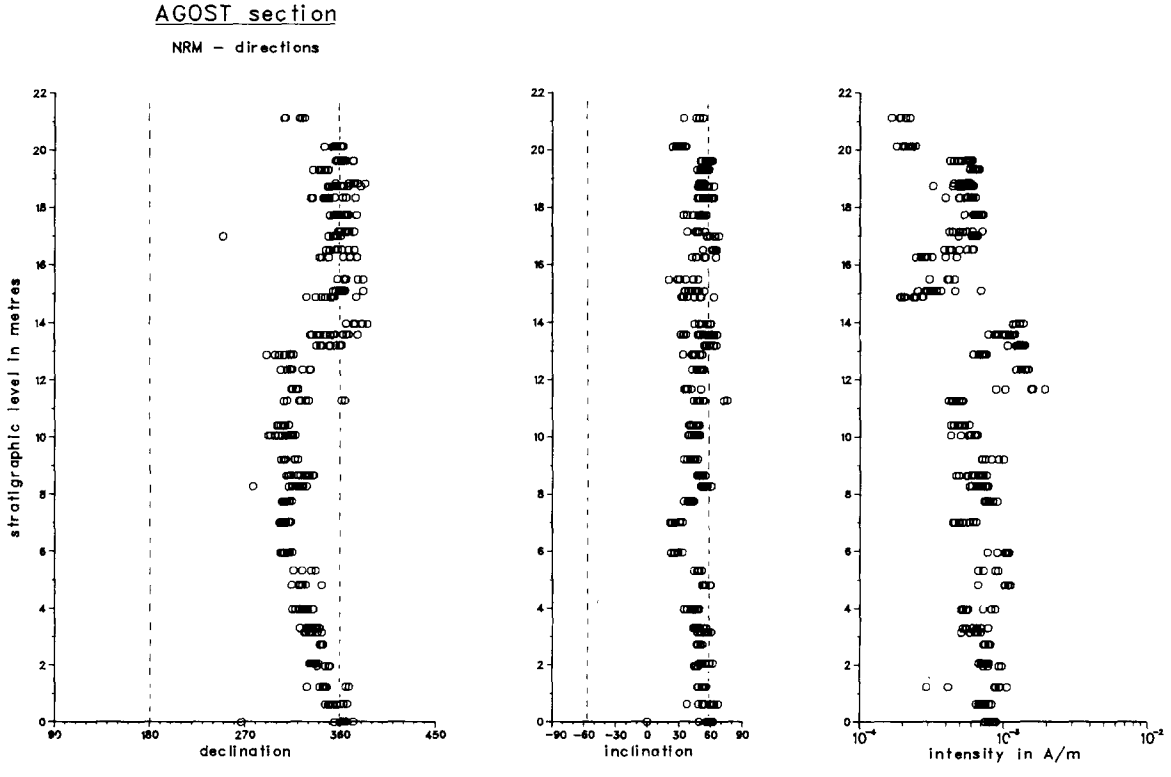

Fig. 3. Declination, inclination of the total NRM of the Agost section, corrected for bedding tilt. Dashed lines represent declination and inclination of the geocentric axial dipole field at the present latitude of the section.

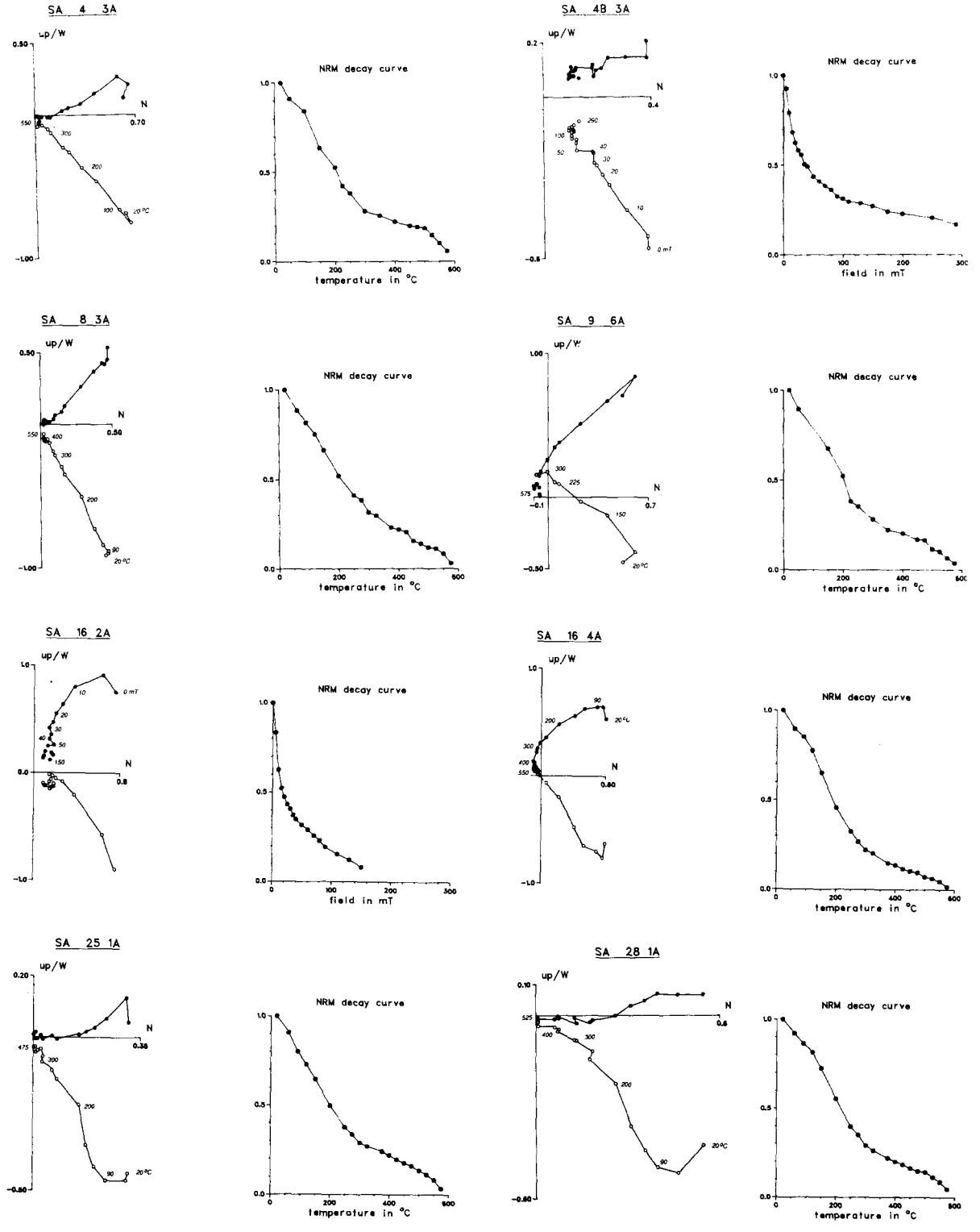

Fig. 4. Representative thermal and alternating field demagnetization diagrams and NRM decay curves of selected samples, corrected for bedding tilt. Generally, the diagrams show three components: a small randomly oriented viscous component is removed at temperatures up to 120 ° C; a relatively large secondary component with a present day direction (if not corrected for bedding tilt) is largely removed at temperatures of ca. 300–350 ° C; a characteristic component is finally removed at temperatures of 575 ° C. Solid (open) circles denote projection on the horizontal (vertical) plane. Numbers refer to temperatures in degrees Celsius or to peak fields in milliTesla (mT). Intensities of the decay curves are normalized.

domly oriented component, which can be removed at temperatures ranging from 50° to 90–120° or with an alternating field of 5 mT. The mostly random orientation and the relatively "soft" character of this component lead to the conclusion that it concerns a laboratory induced viscous magnetization. The second component is a relatively large component, which represents about 60–80% of the original intensity of the specimen. From the thermal decay curves it can be seen that this component is largely removed at temperatures of ca. 300–350 °C. Before bedding tilt correction, this component has a positive inclination and a normal declination with an approximately present-day direction, leading to the conclusion that this component is a secondary magnetization and probably the result of a recent remagnetization due to weathering of the rock. A third component finally is revealed at high temperatures, and it has one of the two characteristic directions; either with a positive inclination and a normal declination or a (shallow) negative inclination and reversed declination (Fig. 4). This third component is the characteristic remanent magnetization (ChRM).

The demagnetization diagrams of, for instance, SA 9 6A and SA 16 4A (Fig. 4) show clearly reversed directions. The inclinations, however, show rather low (negative) values compared to the values of the normal (positive) inclinations. Also, the declinations of the ChRM are not exactly antipodal to those of normal polarity ChRM's. This may indicate that the secondary component is not sufficiently removed and hence that an overlap exists in blocking temperature spectra of the original primary component and the large normal secondary component. Thermal demagnetization of the specimen, however, still succeeds in revealing the polarity of the ChRM, which enables us to use them for magnetostratigraphic purposes.

Whereas thermal demagnetization does reveal the reversed directions, alternating field (AF) demagnetization does not or just marginally. Comparison of the demagnetization diagram of two specimens from the same level (SA 16) shows that the clearly reversed direction of the thermally demagnetized specimen SA 16 4A is not present in the AF demagnetized specimen SA 16 2A (Fig. 4). Further, the AF decay curves do not show the bimodal decay as seen in the thermal decay curves (from ca. 100° to 300–350 °C and from 300–350° to ca. 600 °C; Fig. 4). Also, the different direction of the secondary and characteristic component which is clear from the thermal demagnetization diagrams, cannot be seen in the AF demagnetization diagrams. We conclude that the coercive spectra of the secondary and characteristic magnetizations overlap to an extent that no clear distinction can be made between the two components. Another feature that is sometimes observed is a component with a present-day direction (SA 4B 3A and SA 16 2A) which is not removed at the highest fields (290 mT). This component probably resides in goethite and has a (sub)recent origin due to weathering. In conclusion, alternating field demagnetizations of originally reversed magnetized specimens may easily lead to mis-interpreted normal directions.

Since it is not possible to unequivocably reconstruct the secondary and primary component due to the large spectral overlap, the decay curves in Fig. 4 show the decay of the algebraic sum of the difference vectors between each demagnetization step, rather than interpreting the decay of each component separately (cf. [15]). It appears that about 60–80% of the total intensity has been demagnetized at ca. 350 °C and the resulting 20% diminishes slowly towards the maximum temperature of 575 °C. This means that the magnetic mineral, which carries the secondary component, may reside in maghemite [16], while the magnetic mineral responsible for the ChRM component has maximum blocking temperatures of approximately 575 °C, indicating magnetite as the carrier of this component.

In order to try and gain some more information on the magnetic minerals which are responsible for the various magnetization components of the specimens, the IRM acquisition curves of one specimen per sampling level were determined; the curves of two selected samples are given in Fig. 5. They show that most specimens are not saturated in a direct field of 2 T (e.g. SA 4 2A) and suggest the presence of a high coercive mineral such as goethite. This is confirmed by the continuous thermal demagnetization of the IRM_{max}: ca. 70% of the IRM_{max} is acquired in fields higher than 0.2 T and subsequently removed at 100 °C. The component in the demagnetization diagrams which is not removed at the highest alternating fields is most

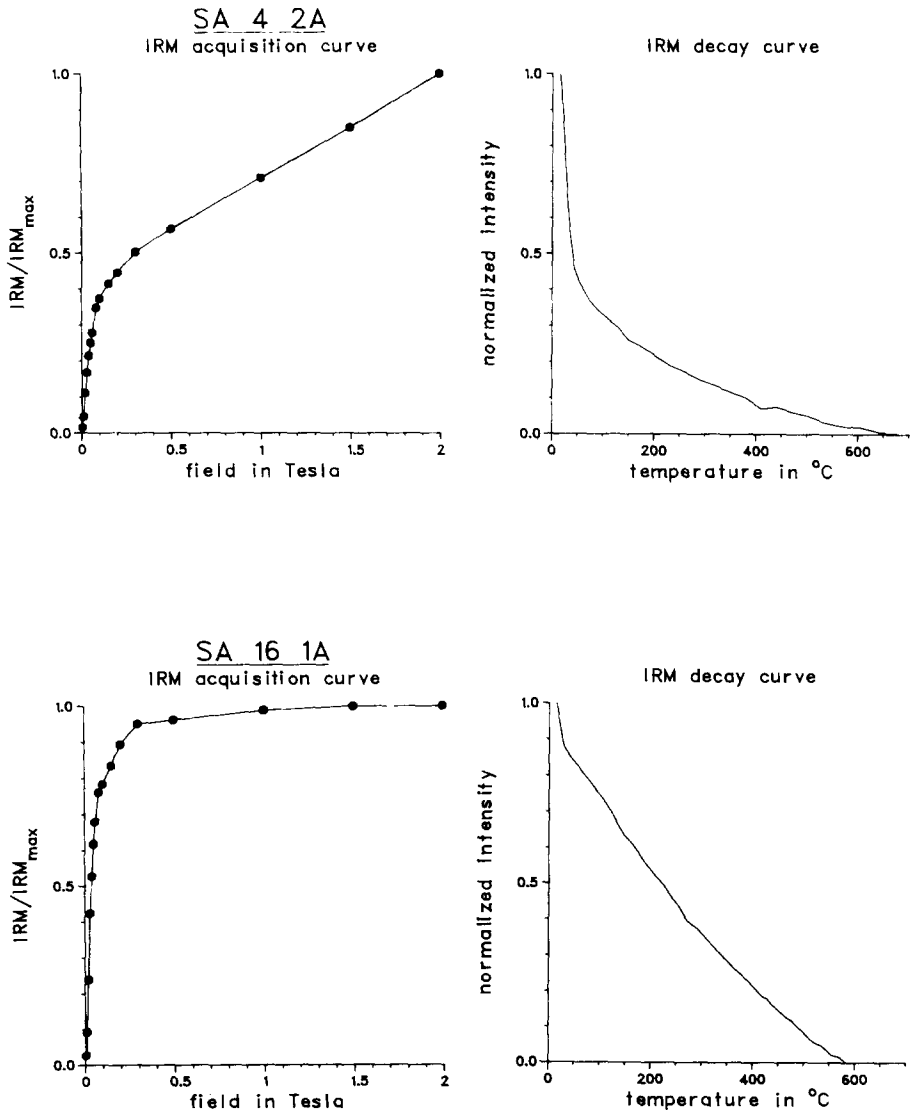

Fig. 5. Normalized isothermal remanent magnetization (IRM) acquisition curves and corresponding continuous thermal decay curves of the maximal IRM. Specimen SA 4 2A does not show saturation in a peak field of 2 T and 60–70% of the maximal IRM is removed at 100 ° C, indicating the presence of goethite. Specimen SA 16 1A shows saturation at 2 T and the maximum blocking temperature of 580 ° C indicates the presence of magnetite.

likely the same component and therefore resides in goethite. Apart from goethite, the IRM acquisition curves and subsequent thermal demagnetization indicate the presence of magnetite with a maximum blocking temperature of 580 ° C (e.g. specimen SA 16 1A).

4.2. Polarity zones

Three polarity zones can cleary be recognized in the directions of the ChRM (Fig. 6). The base of the section is situated within a normal polarity zone. At 6.0 m the first reversed samples occur, the reversal being well defined. The samples taken at 13.6 m show transitional directions and from 14.0 m to the top of the section normal polarities are encountered. On the basis of earlier results [1] the reversed polarity zone is identified as subchron C29r, and hence the lower polarity zone as C30n and the upper normal zone as C29n. The mean directions for the three polarity zones are

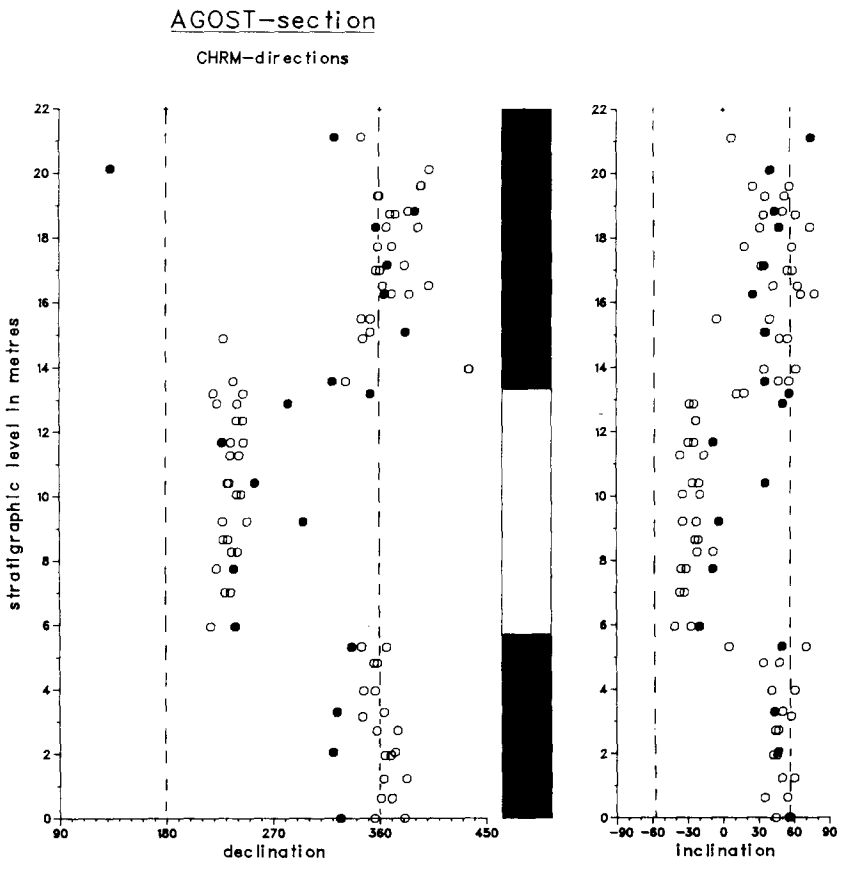

Fig. 6. Declination and inclination of the characteristic remanent magnetization (ChRM) of the Agost section. Open (solid) circles denote results derived from thermal (AF) demagnetization; black (white) denotes normal (reversed) polarity. See also Fig. 3 caption.

from the bottom to the top of the section as follows:

	N	D (°)	I (°)	k	α_{95} (°)
C30n	17	3.8	48.6	61	4.6
C29r	23	235.0	−27.6	72	3.6
C29n	22	13.1	49.7	17	7.6

where N is the numbers of specimens, and k and α_{95} are Fisher's [17] precision parameter and cone of confidence at the 95% level, respectively.

Normal and reversed directions are not antiparallel due to insufficient removal of the large normal secondary overprint (Fig. 7) and therefore it is not realistic to calculate a virtual geomagnetic pole. Also, it can be assumed that the effect of insufficient removal of the secondary component is stronger in the reversed than in the normal ChRM directions and normal and reversed directions may therefore not simply be averaged. The (normal) declinations of the Agost section seem to give an indication for an average clockwise rotation of less than 10°, but the declinations given by VandenBerg and Zijderveld [18] for the Iberian Peninsula show, for the Upper Cretaceous and Lower Tertiary, an anticlockwise rotation of 35°. This difference may be caused by a regional clockwise rotation of the Agost section.

Fig. 8 combines the magnetozonation, biozonation and lithology of the Agost section. The K/T boundary lies within the reversed polarity zone as well as the FAD's of *"Globigerina" eugubina* and *Morozovella pseudobulloides*. The FAD of *Globorotalia trinidadensis* is found at the base of the upper normal polarity zone.

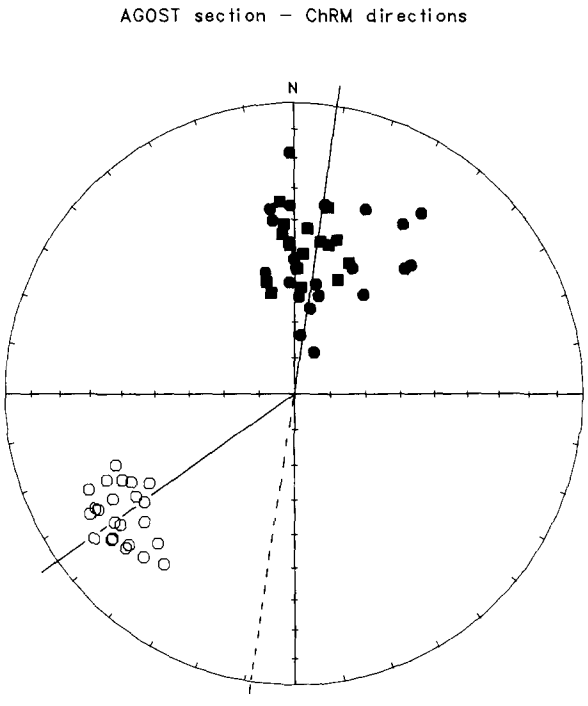

Fig. 7. Equal area projection of ChRM directions from the Agost section. Reversed ChRM directions clearly deviate from normal ChRM direction due to insufficient removal of the secondary (present day) component. Circles refer to directions from chron C29n and C29r, squares to directions from chron C30n; solid (open) symbols denote projection in the lower (upper) sphere.

5. Discussion

In other K/T boundary sections in Europe, such as Gubbio, Zumaya and Caravaca, the K/T boundary occurs at about two thirds from the base Chron 29r. In the Agost section the K/T boundary has been identified at approximately the same level in Chron 29r.

Since the lower boundary of C30n and the upper boundary of C29n were not determined in the Agost section, it was not possible to calculate sedimentation rates for these polarity zones. The average sedimentation rate in C29r is 1.4 cm/ka and linear interpolation would yield an age of 66.33 Ma for the K/T boundary, based on the reversal ages of the Berggren et al. [13] geomagnetic polarity time scale. However, in the sections mentioned above the sedimentation rates of the lower Paleocene are considerably less (by a factor of 3–5) than in the uppermost Cretaceous [6,22].

This change in sedimentation rate is in particular relevant for the Caravaca section, which is bed to bed comparable with the Agost section. In order to estimate the sedimentation rates of the Tertiary and the Cretaceous part of C29r in the Agost section separately, it is necessary to have an estimate of the age of the K/T boundary. Using the ages of the polarity reversals [13] in a linear regression against the lengths of the polarity zones in the Gubbio, Zumaya and Caravaca sections (Fig. 9), we obtain age estimates of 66.45 Ma (Zumaya) and 66.46 Ma (Gubbio) for the K/T boundary based on the Paleocene part and estimates of 66.45 Ma (Caravaca) and 66.78 Ma (Gubbio) based on the Cretaceous part. These results point to an age of 66.45 Ma for the K/T

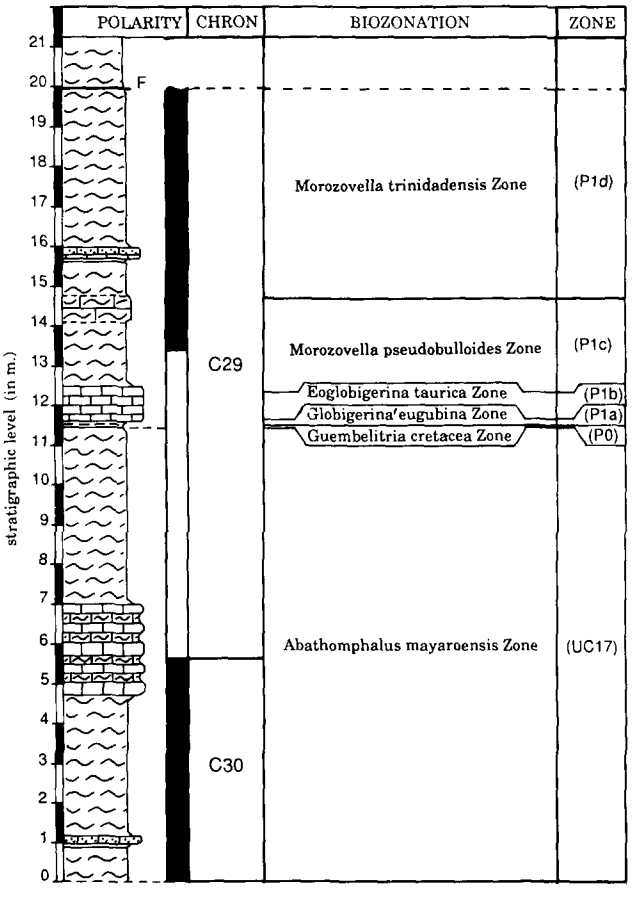

Fig. 8. Combined lithology, magnetostratigraphy and biostratigraphy of the Agost section. Biozonation after [10], chron nomenclature as used by [13]. A fault (*F*) is present in the top of the section.

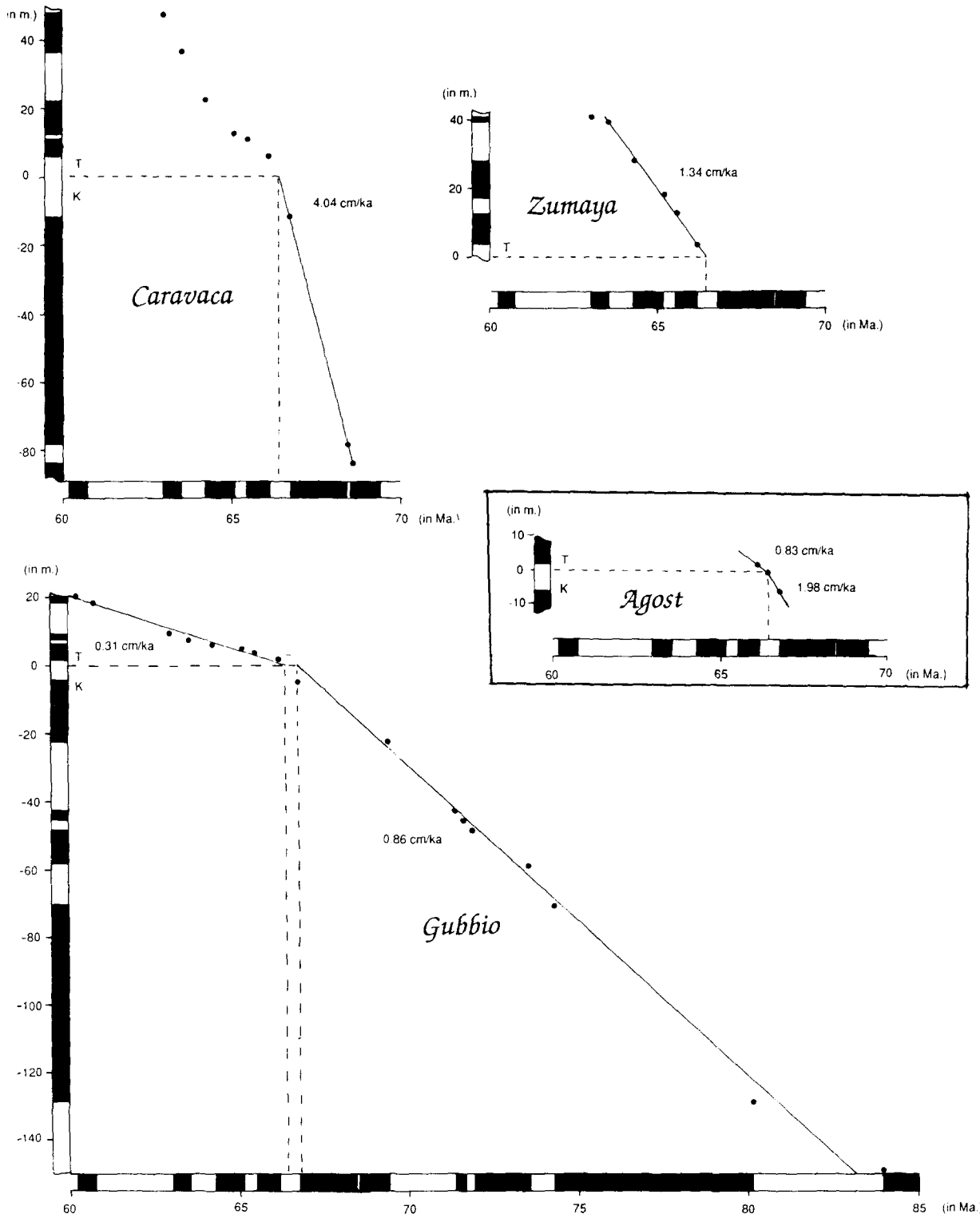

Fig. 9. Sedimentation rates in cm/ka calculated by means of linear regression for the Lower Paleocene and/or Upper Cretaceous in the Gubbio, Zumaya and Caravaca sections, using the polarity time scale of Berggren et al. [13]. The inferred age of 66.45 Ma for the K/T boundary is used to calculate the Upper Cretaceous and Lower Paleocene sedimentation rates in the Agost section.

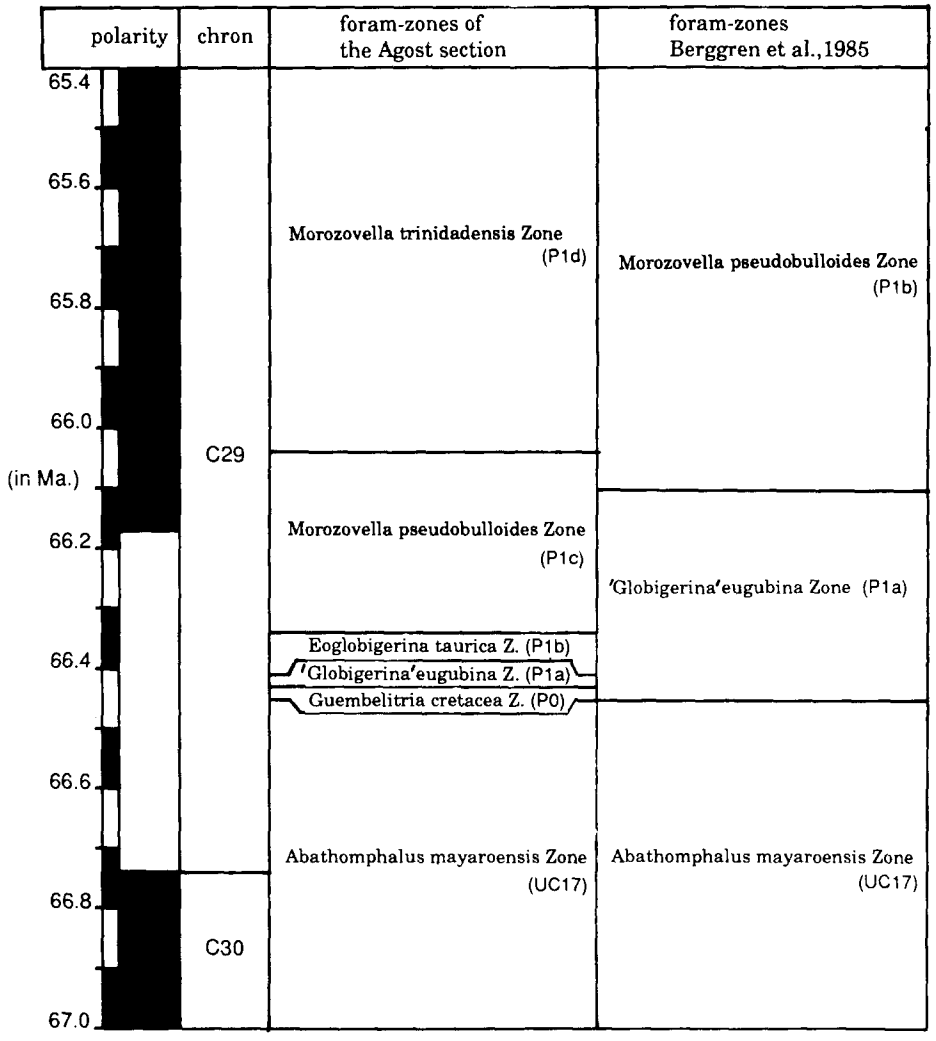

Fig. 10. Linear time scale based on the magnetostratigraphy and the calculated sedimentation rates of the Agost section, compared with the linear time scale of Berggren et al. [13].

boundary, in good agreement with the age of 66.4 Ma given by Berggren et al. [13].

With an age of 66.45 Ma for the K/T boundary the sedimentation rates in the Agost section are 1.98 cm/ka for the Cretaceous part and 0.83 cm/ka for the Tertiary part. A similar decrease in sedimentation rate is seen in the Gubbio and Caravaca sections (Fig. 9). Based on these inferred sedimentation rates, we can evaluate the FAD of early Paleocene marker species (Fig. 10). Berggren et al. [13] do not recognize the *Guembelitria cretacea* Zone (P0) and the ages of the FAD of *"Globigerina" eugubina*, *Morozovella pseudobulloides* and *M. trinidadensis* are younger than the ages calculated for these FAD's of the Agost section.

The FAD's of Berggren et al. [13] are mainly derived from the analysis of thin sections of the Gubbio section. The biozonation of the Agost section is based on a detailed study of washed residues. In washed residues it is much easier to recognize species which occur in relatively low abundance than in thin sections [6]. A FAD of *M. trinidadensis* within C29n is supported by work cited in [13] of Poore et al. [23], Boersma [24], Gerstel et al. [25] and Smit and Romein [10]. Apparently, an abundance of over 2% of a species is required to recognize the same species in thin

sections; if we would have established a biozonation of the Agost section by using frequencies of 2% or higher, there would be better agreement with the timescale of Berggren et al. [13].

The ages of FAD's and the K/T boundary resulting from our investigation of the Agost section are listed below. These ages are estimated by extrapolating accumulation rates of hemipelagic clay, in order to circumvent problems which arise from the carbonate production crisis at the K/T boundary. Obviously, bulk accumulation rates are affected by the fluctuation in carbonate production, leading to deposition of a 6.5 cm thick hemipelagic "boundary" clay on top of the K/T boundary. We have assumed that changes in the influx of clay over the same interval are much less, but we have to admit that we have no independent method to estimate the various accumulation rates involved.

FAD *Morozovella trinidadensis* Bolli	66.04 Ma
FAD *Morozovella pseudobulloides* (Plummer)	66.34 Ma
FAD *Eoglobigerina taurica* (Bang)	66.41 Ma
FAD *"Globigerina" eugubina* Luterbacher & Premoli Silva	66.43 Ma
K/T boundary	66.45 Ma

The time scale of Berggren et al. [13] is used often to estimate rates of extinction and evolution around the K/T boundary. Also, recent estimates of the duration and magnitude of fluxes of e.g. iridium to the seafloor is based on these numbers [20,21]. To improve the accuracy of these calculations it is necessary to have reliable numerical ages, and the present investigation suggests adaptation of numerical details of the widely used Berggren et al. [13] time scale in the early Paleocene.

Acknowledgements

J.D.A. Zijderveld critically read earlier versions of the manuscript.

References

1 W. Alvarez, M.A. Arthur, A.G. Fischer, W. Lowrie, G. Napoleone, I. Premoli Silva and W.M. Roggenthen, Upper Cretaceous–Paleocene magnetic stratigraphy at Gubbio, Italy, Geol. Soc. Am. Bull. 88, 367–389, 1977.

2 L.W. Alvarez, W. Alvarez, F. Asaro and H. Michel, Extraterrestrial cause for the Cretaceous Tertiary extinction, Sience 280, 1095–1108, 1980.

3 J. Smit and J. Hertogen, An extraterrestrial event at the Cretaceous–Tertiary boundary, Nature 285, 198–200, 1980.

4 W. Lowrie, W. Alvarez, G. Napoleone, K. Perch-Nielsen, I. Premoli Silva and M. Tourmakine, Paleocene magnetic stratigraphy in Umbrian pelagic carbonate rocks: Contessa sections, Gubbio, Geol. Soc. Am. Bull. 93, 414–432, 1982.

5 W.M. Roggenthen, Magnetic stratigraphy of the Paleocene: a comparison between Spain and Italy, Mem. Soc. Geol. Ital. 15, 73–82, 1976.

6 J. Smit, Extinction and evolution of planktonic foraminifera after a major impact at the Cretaceous–Tertiary boundary, Geol. Soc. Am. Spec. Pap. 190, 329–352, 1982.

7 A. von Hillebrandt, Paleogene biostratigraphy in southeastern Spain (Murcia and Alicante Provinces), Actes du VI Coll. Africain de Micropaléontologie (Tunis), pp. 231–248, 1974.

8 W. Kampschuur and H.E. Rondeel, The origin of the Betic Orogen, Southern Spain, Tectonophysics 27, 39–56, 1975.

9 C.G. Langereis and J.E. Meulenkamp, Comparison of two methods to measure lithostratigraphical intervals in sections Potamida 1 and 2, Utrecht, Micropaleontol. Bull. 21, 23–26, 1979.

10 J. Smit and A.J.T. Romein, A sequence of events across the Cretaceous–Tertiary boundary, Earth Planet. Sci. Lett., 74, 155–170, 1985.

11 J.E. van Hinte, A Cretaceous time scale, Am. Assoc. Pet. Geol. Bull. 60, 498–516, 1976.

12 J. Hardenbol and W.A. Berggren, A new Paleogene numerical time scale, Am. Assoc. Pet. Geol., Stud. Geol. 6, 213–234, 1978.

13 W.A. Berggren, D.V. Kent and J.J. Flynn, Paleogene geochronology and chronostratigraphy, in: The Chronology of the Geological Record, N.J. Snelling, ed., Geol. Soc. London Mem. 10, 141–195, 1985.

14 J.D.A. Zijderveld, A.C. demagnetization of rocks: analysis of results, in: Methods in Palaeomagnetism, D.W. Collinson et al., eds., pp. 254–286, Elsevier, Amsterdam, 1967.

15 C.G. Langereis, Late Miocene magnetostratigraphy in the Mediterranean, Ph.D. Thesis, University of Utrecht, 1984.

16 P.H.M. Dankers, Magnetic properties of dispersed natural iron-oxides of known grain size, Ph.D. Thesis, University of Utrecht, 1978.

17 R. Fisher, Dispersion on a sphere, Proc. R. Soc. London, Ser. A 217, 295–305, 1953.

18 J. VandenBerg and J.D.A. Zijderveld, Paleomagnetism in the Mediterranean area, Alpine Med. Geodyn., Geodyn. Ser. 7, 83–112, 1982.

19 A. von Hillebrandt, Foraminiferen Stratigraphie im Alt Tertiär von Zumaya (Prov. de Guipuzcoa, NW Spanien), Bayer. Akad. Wiss., Abh. N.F. 123, 1–63, 1965.

20 C.B. Officer and C.L. Drake, The Cretaceous–Tertiary transition, Sience 219, 1383–1390, 1983.

21 C.B. Officer and C.L. Drake, 1985. Terminal Cretaceous environmental events, Sience 227, 1161–1167, 1985.

22 D.V. Kent, An estimate of the duration of the faunal change at the Creataceous–Tertiary boundary, Geology 5, 769–771, 1977.

23 R.Z. Poore, L. Tauxe, S.F. Percival, Jr., J.L. LaBrecque, R. Wright, N.P. Petersen, C.C. Smith, P. Tucker and K.J. Hsü, Late Cretaceous–Cenozoic magnetostratigraphy and bio-

stratigraphic correlations of the South Atlantic Ocean, in: K.J. Hsü, J.L. LaBrecque et al., Init. Rep. DSDP 73, 645–656, 1984.

24 A. Boersma, Cretaceous–Tertiary Planktonic foraminifers from the South Eastern Atlantic, Walvis Ridge Area, Deep Sea Drilling Project Leg 74, in: T.C. Moore, Jr., P.D. Rabinowitz et al., Init. Rep. DSDP 74, 501–524, 1984.

25 J.Gerstel, R.C. Thunell, J.C. Zachos and M.A. Arthur, The Cretaceous–Tertiary boundary event in the North Pacific: planktonic foraminiferal results from Deep Sea Drilling Project Site 577, Shatsky Rise, Paleoceanography 1, 97–117, 1986.